Insulin/Insulin-like Growth Factor I Hybrid Receptors Have Different Biological Characteristics Depending on the Insulin Receptor Isoform Involved*

Giuseppe Pandini‡§¶, Francesco Frasca‡‖, Rossana Mineo‡‖, Laura Sciacca‡, Riccardo Vigneri‡§, and Antonino Belfiore‡‡**

*From the ‡Istituto di Medicina Interna, Malattie Endocrine e del Metabolismo, University of Catania, Ospedale Garibaldi, 95123 Catania, Italy, the §Istituto Mediterraneo di Oncologia, 95100 Catania, Italy, and the **Dipartimento di Medicina Clinica e Sperimentale, University of Catanzaro, Policlinico Mater Domini, via T. Campanella 115, 88100 Catanzaro, Italy*

The insulin receptor (IR) and the insulin-like growth factor I receptor (IGF-IR) have a highly homologous structure, but different biological effects. Insulin and IGF-I half-receptors can heterodimerize, leading to the formation of insulin/IGF-I hybrid receptors (Hybrid-Rs) that bind IGF-I with high affinity. As the IR exists in two isoforms (IR-A and IR-B), we evaluated whether the assembly of the IGF-IR with either IR-A or IR-B moieties may differently affect Hybrid-R signaling and biological role. Three different models were studied: (*a*) 3T3-like mouse fibroblasts with a disrupted IGF-IR gene (R⁻ cells) cotransfected with the human IGF-IR and with either the IR-A or IR-B cDNA; (*b*) a panel of human cell lines variably expressing the two IR isoforms; and (*c*) HepG2 human hepatoblastoma cells predominantly expressing either IR-A or IR-B, depending on their differentiation state. We found that Hybrid-Rs containing IR-A (Hybrid-Rs^A) bound to and were activated by IGF-I, IGF-II, and insulin. By binding to Hybrid-Rs^A, insulin activated the IGF-I half-receptor β-subunit and the IGF-IR-specific substrate CrkII. In contrast, Hybrid-Rs^B bound to and were activated with high affinity by IGF-I, with low affinity by IGF-II, and insignificantly by insulin. As a consequence, cell proliferation and migration in response to both insulin and IGFs were more effectively stimulated in Hybrid-R^A-containing cells than in Hybrid-R^B-containing cells. The relative abundance of IR isoforms therefore affects IGF system activation through Hybrid-Rs, with important consequences for tissue-specific responses to both insulin and IGFs.

The insulin receptor (IR)[1] and the insulin-like growth factor (IGF) I receptor (IGF-IR) are tetrameric glycoproteins composed of two extracellular α- and two transmembrane β-subunits linked by disulfide bonds. Each α-subunit, containing the ligand-binding site, is ~130 kDa, whereas each β-subunit, containing the tyrosine kinase domain, is ~95–97 kDa. These receptors share >50% overall amino acid sequence homology and 84% homology in the tyrosine kinase domains. After ligand binding, activated receptors recruit and phosphorylate docking proteins, including the insulin receptor substrate-1 family proteins Gab1 and Shc (1–5), leading to the activation of many intracellular mediators, including phosphatidylinositol 3-kinase, Akt, and ERK1/2, involved in the regulation of cell metabolism, proliferation, and survival. Although both the IR and IGF-IR similarly activate major signaling pathways, subtle differences exist in the recruitment of certain docking proteins and intracellular mediators between the two receptors (6–9). These differences are the basis for the predominant metabolic effect elicited by IR activation and the predominant mitogenic, transforming, and anti-apoptotic effect elicited by IGF-IR activation (10–13). According to the classical view, insulin binds with high affinity to the IR (100-fold higher than to the IGF-IR), whereas both insulin-like growth factors (IGF-I and IGF-II) bind to the IGF-IR (with 100-fold higher affinity than to the IR).

Given the high degree of homology, the insulin and IGF-I half-receptors (composed of one α- and one β-subunit) can heterodimerize, leading to the formation of insulin/IGF-I hybrid receptors (Hybrid-Rs) (14–16). In many tissues, Hybrid-Rs are the most represented receptor subtype (17). Hybrid-Rs may also be overexpressed in a variety of human malignancies as a result of both IR and IGF-IR overexpression (18–21). However, the biological role of these Hybrid-Rs is still unclear. Functional studies have indicated that Hybrid-Rs behave more like IGF-IRs than IRs because they bind to and are activated by IGF-I with an affinity similar to that of the typical IGF-IR. In contrast, Hybrid-R activation in response to insulin occurs with much lower affinity (22, 23). Hybrid-Rs are therefore believed to provide additional binding sites to IGF-I and to increase cell sensitivity to this growth factor (17–19). These studies have not, however, taken into account the different IR isoform contribution to Hybrid-R formation and function.

The human IR exists in two isoforms (IR-A and IR-B), gen-

[1] The abbreviations used are: IR, insulin receptor; IGF, insulin-like growth factor; IGF-IR, insulin-like growth factor I receptor; ERK, extracellular signal-regulated kinase; Hybrid-R, insulin/insulin-like growth factor I hybrid receptor; Hybrid-R^A, insulin/insulin-like growth factor I hybrid receptor containing the insulin receptor A isoform; Hybrid-R^B, insulin/insulin-like growth factor I hybrid receptor containing the insulin receptor B isoform; BSA, bovine serum albumin; PMSF, phenylmethylsulfonyl fluoride; BrdUrd, bromodeoxyuridine; ELISA, enzyme-linked immunosorbent assay; GFP, green fluorescent protein; PBS, phosphate-buffered saline; RT, reverse transcription; X-gal, 5-bromo-4-chloro-3-indolyl-β-D-galactopyranoside; SH, Src homology.

erated by alternative splicing of the insulin receptor gene that either excludes or includes 12 amino acid residues encoded by a small exon (exon 11) at the carboxyl terminus of the IR α-subunit (see Table I). The relative abundance of IR isoforms is regulated by tissue-specific and unknown factors (24, 25). Recently, we found that IR-A (but not IR-B) binds IGF-II with high affinity and behaves as a second physiological receptor for IGF-II in fetal and dedifferentiated (malignant) cells (26–28). We therefore hypothesized that the relative abundance of the two isoforms may affect the functional properties of Hybrid-Rs and modulate, in this way, the activation of the IGF system.

To investigate these issues, we used three different cellular models. First, we used R$^-$ fibroblasts, which are 3T3-like cells derived from IGF-IR knockout mice. These cells also have low levels of endogenous IR. We cotransfected these cells with both the human IGF-IR gene and a construct encoding either IR-A or IR-B to obtain cells expressing either Hybrid-Rs^A or Hybrid-Rs^B, respectively (see Table I). Second, we employed a panel of human cell lines that express the two IR isoforms in variable amounts. Third, we used HepG2 hepatoblastoma cells that express predominantly either IR-A or IR-B depending on the culture conditions (29).

We found that each of the IR isoforms is equally able to form hybrids with the IGF-IR. Hybrid-Rs^A and Hybrid-Rs^B, however, have different functional characteristics. Hybrid-Rs^B have a high affinity only for IGF-I. Hybrid-Rs^A have an even higher affinity for IGF-I and bind also IGF-II and insulin. Insulin binding to Hybrid-Rs^A phosphorylates the IGF-IR β-subunit and activates CrkII, an IGF-IR-specific substrate. Accordingly, cell transfection with IR-A cDNA (but not with IR-B cDNA) markedly increases cell motility in response not only to IGF-I, but also to insulin and IGF-II.

These data therefore suggest that the relative abundance of IR isoforms modulates the activation of the IGF system by regulating both binding and signaling characteristics of Hybrid-Rs. They also provide clues to the mechanism by which insulin may activate the IGF-IR phosphorylation cascade and biological effects in a tissue-specific manner. These findings may have important implications for cell biological responses to insulin, IGF-I, and IGF-II.

EXPERIMENTAL PROCEDURES
Materials

The pNTK2 expression vectors containing the cDNAs for the A (Ex11$^-$) and B (Ex11$^+$) isoforms of the human IR were kindly provided by Dr. Axel Ullrich (Max Planck Institute of Biochemistry, Martinsried, Germany). The pECE expression vector containing the cDNA encoding the human IGF-IR was a gift of Dr. R. Roth (Department of Molecular Pharmacology, Stanford University, Stanford, CA). The pCH110 expression vector for β-galactosidase was kindly provided by Dr. F. Tatò (Universitá di Roma "La Sapienza," Rome, Italy). The expression vector for pBOS-H2B-GFP was kindly provided by Dr. J. Y. Wang (University of California at San Diego, San Diego, CA).

The following materials were purchased from the indicated manufacturers: fetal calf serum, glutamine, LipofectAMINE, and DNase I from Invitrogen (Paisley, UK); RPMI 1640 medium, Dulbecco's modified Eagle's medium, minimum essential medium, Ham's nutrient mixture F-12, bovine serum albumin (BSA; radioimmunoassay grade), bacitracin, phenylmethylsulfonyl fluoride (PMSF), puromycin, bromodeoxyuridine (BrdUrd), and porcine insulin from Sigma; protein G-Sepharose from Amersham Biosciences (Uppsala, Sweden); and ^{125}I-labeled IGF-I (specific activity of 11.1 MBq/μg) from PerkinElmer Life Sciences (Zaventem, Belgium). IGF-I and IGF-II were obtained from Calbiochem, and FuGENE 6 transfection reagent was obtained from Roche Molecular Biochemicals (Mannheim, Germany).

The following anti-IR antibodies were employed: monoclonal antibodies MA-10 and MA-20 (which recognize the IR α-subunit, but only poorly recognize the Hybrid-R) (Dr. I. D. Goldfine, University of California at San Francisco, San Francisco, CA) (30, 31); monoclonal antibody CT-1 (which recognizes the IR β-subunit) and monoclonal antibody 83-7 (which recognizes the α-subunits of both the IR and Hybrid-R) (Dr.

TABLE I
Description of receptors and tranfected cells studied

	Description
Receptors	
IR-A	IR isoform lacking 12 amino acid residues encoded by exon 11
IR-B	IR isoform containing 12 amino acid residues encoded by exon 11
Hybrid-R^A	Receptor composed of one α- and one β-subunit of the IGF-IR and one α- and one β-subunit of IR-A
Hybrid-R^B	Receptor composed of one α- and one β-subunit of the IGF-IR and one α- and one β-subunit of IR-B
Cells	
R$^-$	3T3-like fetal fibroblasts derived from IGF-IR knockout mice
R$^-$IR-A	R$^-$ cells transfected with a construct encoding IR-A
R$^-$IR-B	R$^-$ cells transfected with a construct encoding IR-B
R$^+$	R$^-$ cells transfected with the human IGF-IR gene
R$^+$A	R$^+$ cells transfected with a construct encoding IR-A to obtain cells expressing the Hybrid-R^A
R$^+$B	R$^+$ cells transfected with a construct encoding for IR-B to obtain cells expressing the Hybrid-R^B

K. Siddle, University of Cambridge, Cambridge, UK) (32, 33); a rabbit polyclonal antibody that recognizes the IR β-subunit (Transduction Laboratories, Lexington, KY); and polyclonal antibody 29B4 (which recognizes the IR β-subunit) (Santa Cruz Biotechnology Inc., Santa Cruz, CA).

The following anti-IGF-IR antibodies were employed: monoclonal antibody αIR-3 (which recognizes the IGF-IR α-subunit and only poorly recognizes the Hybrid-R) (Oncogene Research, Cambridge, MA) (34); monoclonal antibody 17-69 (which recognizes the α-subunits of both the IGF-IR and Hybrid-R) (Dr. K. Siddle) (35); and a chicken polyclonal antibody that recognizes the IGF-IR α-subunit (Upstate Biotechnology, Inc., Lake Placid, NY). Anti-phospho-ERK1/2 and anti-phospho-Akt antibodies were purchased from New England Biolabs (Beverly, MA); anti-phosphotyrosine monoclonal antibody 4G10 was from Upstate Biotechnology, Inc.; and anti-BrdUrd antibody was from BD PharMingen (Erembodegem, Belgium).

Cells

ARO cells were kindly provided by Dr. A. Pontecorvi (Regina Elena Cancer Institute, Rome, Italy). A549, IM-9, HepG2, MDA-MB157, and PC-3 cells were obtained from American Type Culture Collection. R$^-$ mouse fibroblasts (3T3-like mouse cells derived from animals with a targeted disruption of the IGF-IR gene, expressing $\sim$5 $\times$ 10^3 insulin receptors/cell) were kindly provided by Dr. R. Baserga (Kimmel Cancer Center, Jefferson University, Philadelphia, PA) (Table I). HepG2 and MDA-MB157 cells were routinely grown in minimum essential medium supplemented with 10% fetal bovine serum. A549, PC-3, IM-9 and ARO cells were routinely grown in RPMI 1640 medium supplemented with 10% fetal bovine serum. The R$^-$ mouse fibroblasts were routinely grown in Dulbecco's modified Eagle's medium supplemented with 10% fetal bovine serum.

Transfection Experiments

R$^-$ cells were grown in 35-mm plates until 60–70% confluent. They were first transfected with 2 μg of pECE expression vector containing the cDNA encoding the IGF-IR (36) and cotransfected with 0.2 μg of pSV2 plasmid encoding the hygromycin resistance gene by the LipofectAMINE method according to the manufacturer's protocol. Cells were then subjected to antibiotic selection in medium supplemented with 400 μg/ml hygromycin for 3 weeks. Stably transfected clones were tested for receptor content by ELISA. Cell clones were further transfected with the pNTK2 expression vector containing the cDNA for either the A (Ex11$^-$) or B (Ex11$^+$) isoform of the human IR (37) and cotransfected with the pPDV6$^+$ plasmid encoding the puromycin resistance gene. Cells were subsequently subjected to antibiotic selection in medium supplemented with 400 μg/ml hygromycin and 2.4 μg/ml puromycin for 3 weeks. Receptor content was evaluated in selected clones by ELISA. Cell clones expressing similar amounts of either IR-A or IR-B, IGF-IR, and Hybrid-R (either the Hybrid-R^A or Hybrid-R^B) were selected for subsequent studies. For migration studies, HepG2 cells were transiently transfected by the FuGENE 6 method according to the manufacturer's protocol. Briefly, 4 $\times$ 10^5 cells were seeded in six-well plates and grown for 24 h in complete medium (minimum essential medium with 10% fetal bovine serum). Thereafter, a transfection mix-

ture containing 2 μg of pNTK2-IR-A/IR-B + 0.2 μg of β-galactosidase or histone H2B-GFP + 12 μl of FuGENE 6 in 100 μl of minimal essential medium without serum or antibiotics was added to each well. Cells were grown in complete medium; and after 48 h, they were assayed for β-galactosidase activity or scored under a fluorescence microscope for GFP expression.

Preparation of Cell Lysate

Cells were grown until 80% confluent and serum-starved 24 h before stimulation with the various ligands. For receptor and ERK/Akt activation, cells were stimulated with 10 nM insulin, IGF-I, or IGF-II for 10 min. For *in vitro* Crk phosphorylation, cells were stimulated with 50 nM insulin, IGF-I, or IGF-II for 5 min. After three washes with ice-cold PBS, cells were lysed in cold radioimmune precipitation assay buffer containing 50 mM Tris (pH 7.4), 150 mM NaCl, 0.5% Nonidet P-40, 0.5% Triton X-100, 0.25% sodium deoxycholate, 10 mM sodium pyrophosphate, 1 mM NaF, 1 mM sodium orthovanadate, 2 mM PMSF, 10 μg/ml aprotinin, 10 μg/ml pepstatin, and 10 μg/ml leupeptin. After being scraped, samples were rotated for 15 min at 4 °C. Insoluble material was separated from the soluble extract by microcentrifugation at 10,000 $\times$ g for 10 min at 4 °C. Protein concentration was determined by the Bradford assay.

Ligand Binding Assay for the Hybrid-R^A or Hybrid-R^B

Either the Hybrid-R^A or Hybrid-R^B was captured by incubating cell lysates for 22 h in Maxisorp Break-Apart immunoplates (Nunc, Roskilde, Denmark) precoated with 2 μg/ml antibody 83-7. After washing, the immunocaptured receptors were incubated with ^{125}I-labeled IGF-I (10 pM in 50 mM HEPES-buffered saline (pH 7.6) containing 0.05% Tween 20, 1% BSA, 2 mM sodium orthovanadate, 1 mg/ml bacitracin, and 1 mM PMSF) in the presence or absence of increasing concentrations of various unlabeled ligands (insulin, IGF-I, and IGF-II). After 2 h at room temperature, the plates were washed, and the radioactivity in each well was counted in a γ-counter.

IR, IGF-IR, and Hybrid-R Measurements

Cell lysates were prepared as described above and used for receptor measurement both by ELISA and Western blot analysis.

ELISA—The characteristics and specificity of these ELISAs have been previously described (18). Receptors were captured by incubating lysates (0.5–60 μg/well) in Maxisorp immunoplates precoated with the specific monoclonal antibody (2 μg/ml) indicated below. After washing, the immunocaptured receptors were incubated with the specific biotinylated monoclonal antibody indicated below (0.3 μg/ml in 50 mM HEPES-buffered saline (pH 7.6) containing 0.05% Tween 20, 1% BSA, 2 mM sodium orthovanadate, 1 mg/ml bacitracin, and 1 mM PMSF) and then with peroxidase-conjugated streptavidin. The peroxidase activity was determined colorimetrically by adding 100 μl of 3,3′,5,5′-tetramethylbenzidine (0.4 mg/ml in 0.1 M citrate/phosphate buffer (pH 5.0) with 0.4 μl/ml 30% H_2O_2). The reaction was stopped by the addition of 1.0 M H_3PO_4, and the absorbance was measured at 450 nm.

IRs were captured with anti-IR antibody MA-20 and detected with biotinylated anti-IR antibody CT-1 (30, 33). IGF-IRs were captured with anti-IGF-IR antibody αIR-3 and detected with biotinylated antibody 17-69 (34, 35). Hybrid-Rs were captured with anti-IR antibody 83-7, which recognizes both the Hybrid-R and IR, and detected with biotinylated anti-IGF-IR antibody 17-69 (32, 35). The receptor content was evaluated by comparing each sample with a standard curve, as previously described (18).

The minimal detectable amount of hybrids was 0.125 ng/well (1.25 ng/ml). The assay was linear from 0.125 to 1.0 ng/well. There was no interference from either 1 ng/well purified IR (from human IR cDNA-transfected NIH/3T3 cells) or 1 ng/well purified IGF-IR (from human IGF-IR cDNA-transfected Chinese hamster ovary cells). Multiple dilutions of cells and tissues containing either Hybrid-Rs^A or Hybrid-Rs^B produced dose-response curves parallel to those obtained with the purified IR/IGF-IR hybrid standard (Ref. 18 and data not shown). Intra-assay coefficients of variation were <7% at 0.5 ng/tube and <8% at 1.0 ng/tube. Inter-assay coefficients of variation were <8 and <10%, respectively (18).

The ELISAs for the IR and IGF-IR had similar characteristics of sensitivity and specificity, as previously described (18). Purified IGF-IR or Hybrid-R (up 1 ng/well) did not interfere in the IR assay, and purified IR or Hybrid-R did not interfere in the IGF-IR assay. The minimal detectable amounts were 0.05 ng/tube for the IR and 0.0625 ng/tube for the IGF-IR. Intra-assay coefficients of variation were <8%, and inter-assay coefficients of variation were <10% for both assays (18).

Western Blotting—To confirm data obtained by ELISA, aliquots of the same lysates were subjected to Western blot analysis. Cell lysates were incubated at 4 °C under constant rotation for 2 h with 4 μg of the specific anti-receptor antibody and then for 2 h with protein G-Sepharose. Immunoprecipitates were eluted and subjected to SDS-PAGE and then immunoblotted (1 μg/ml) as described below. IRs were immunoprecipitated with anti-IR antibody MA-20 and blotted with the rabbit anti-IR polyclonal antibody. IGF-IRs were immunoprecipitated with anti-IGF-IR antibody αIR-3 and blotted with the chicken anti-IGF-IR polyclonal antibody. Hybrid-Rs were immunoprecipitated with anti-IR antibody 83-7 and blotted with the chicken anti-IGF-IR polyclonal antibody. Western blot specificity was evaluated by examining the interference of 200 ng of purified receptor of each subtype added to a cell lysate containing ~200 ng of IR, IGF-IR, or Hybrid-R.

Hybrid-R Autophosphorylation

Western Blotting—Cell lysates were incubated at 4 °C under constant rotation for 1 h with protein G-Sepharose to eliminate antibody MA-10 bound to the IR. After centrifugation, the supernatant was incubated at 4 °C under constant rotation for 2 h with 4 μg of anti-Hybrid-R antibody 83-7 coated with protein G-Sepharose. Immunoprecipitates were eluted and subjected to SDS-PAGE. The resolved proteins were transferred to nitrocellulose membranes, immunoblotted with anti-phosphotyrosine monoclonal antibody 4G10, and revealed by an ECL method. The nitrocellulose membrane was then stripped with Restore stripping buffer (Pierce) for 30 min at room temperature and subsequently reprobed with the chicken anti-IGF-IR polyclonal antibody.

ELISA—As previously described (38), 100 μl of the cell lysates prepared as described above were immunocaptured in Maxisorp plates coated with antibodies 83-7 (which recognizes both the IR and Hybrid-R) and MA-20 (which recognizes the IR only) at a concentration of 2 μg/ml in 50 mM sodium bicarbonate (pH 9.0) overnight at 4 °C. After washing, the captured phosphorylated proteins were incubated with biotin-conjugated anti-phosphotyrosine antibody 4G10 (0.3 μg/ml in 50 mM HEPES (pH 7.6), 150 mM NaCl, 0.05% Tween 20, 1% BSA, 2 mM sodium orthovanadate, 1 mg/ml bacitracin, and 1 mM PMSF) for 2 h at 22 °C and then with peroxidase-conjugated streptavidin. The peroxidase activity was determined colorimetrically by adding 100 μl of 3,3′,5,5′-tetramethylbenzidine (0.4 mg/ml in 0.1 M citrate/phosphate buffer (pH 5.0) with 0.4 μl/ml 30% H_2O_2). The reaction was stopped by the addition of 1.0 M H_3PO_4, and the absorbance was measured at 450 nm.

In Vitro CrkII Phosphorylation

In vitro receptor tyrosine kinase activity for CrkII was measured as previously described (9) with modifications. 500 μg of proteins were immunoprecipitated with either anti-IR monoclonal antibody MA-20 or anti-Hybrid-R antibody 83-7 coupled to protein G-Sepharose. Pellets were washed twice with radioimmune precipitation assay buffer and twice with kinase buffer without ATP and resuspended in 100 μl of kinase buffer containing 50 mM HEPES (pH 7.4), 150 mM NaCl, 0.1% Triton X-100, 10 mM $MgCl_2$, 2 mM $MnCl_2$, 0.05% BSA, 50 μM ATP, and 1 μg of glutathione *S*-transferase-Crk (provided by Dr. Raymond Birge, Rockefeller University). Reaction mixtures were incubated at room temperature for 20 min under continuous agitation. After rapid centrifugation at 14,000 rpm, supernatants were collected, and 4$\times$ sample buffer was added. Samples were boiled for 3 min; subjected to SDS-PAGE; and transferred to nitrocellulose membranes, which were blotted with anti-phosphotyrosine antibody 4G10. Membranes were stripped and reprobed with anti-CrkII polyclonal antibody (Santa Cruz Biotechnology Inc.) where required.

ERK1/2 and Akt Phosphorylation in Response to Insulin, IGF-I, or IGF-II

After the addition of 5$\times$ sample buffer, samples were heated at 95–100 °C for 5 min and subjected to reducing SDS-PAGE on 10% polyacrylamide gel. After electrophoresis, the resolved proteins were transferred to nitrocellulose membranes and subjected to immunoblot analysis. For ERK1/2 activation studies, the blots were probed with the phospho-specific ERK1/2 polyclonal antibody. For Akt phosphorylation studies, the blots were probed with anti-phospho-Akt antibody. The nitrocellulose membranes were then stripped with stripping buffer for 30 min at room temperature and subsequently reprobed with either anti-ERK1/2 polyclonal antibody or anti-Akt polyclonal antibody. All immunoblots were revealed by the ECL method, autoradiographed, and subjected to densitometric analysis.

IR, IGF-IR, and Hybrid-R content in cell clones obtained from R^- fibroblasts transfected with the IGF-IR and with either the IR-A (clones A28, A25, and A48) or IR-B (clones B15, B22, and B3) cDNA

Clones A25 and B22, with a similar receptor content, were selected for subsequent studies. Data represent mean ± S.E. of three different experiments.

Clones	Receptor content			
	IR	IGF-IR	Hybrid-R	
			Measured	Predicted[a]
		ng/100 µg protein		
R⁺A28	11.0 ± 0.8	5.4 ± 0.3	24.2 ± 1.5	15.4
R⁺A25	18.4 ± 1.2	6.8 ± 0.4	21.8 ± 2.2	22.4
R⁺A48	25.1 ± 1.1	5.6 ± 0.7	28.6 ± 3.2	23.7
R⁺B15	12.3 ± 1.2	8.5 ± 0.6	19.3 ± 2.3	20.4
R⁺B22	18.2 ± 0.7	7.2 ± 0.9	22.4 ± 1.6	22.9
R⁺B3	20.6 ± 1.7	9.3 ± 0.6	24.5 ± 2.8	27.7

[a] If the total concentrations of insulin and IGF-I half-receptors are I and G, respectively, and these half-receptors combine randomly, then it would be predicted that the relative concentrations of IR/IGF-IR/Hybrid-R would be $I^2:G^2:2IG$. Thus, the measured content of Hybrid-Rs can be compared with the expected content on the basis of random assembly, since Hybrid-Rs = $2 \cdot \sqrt{IR} \cdot \sqrt{IGF-IR}$.

IR Isoform RT-PCR

RT-PCR for IR isoforms was carried out as previously described (39) using oligonucleotide primers spanning nucleotides 2230–2251 (5′-AAC-CAG-AGT-GAG-TAT-GAG-GAT-3′) and 2846–2867 (accession M10051) (5′-CCG-TTC-CAG-AGC-GAA-GTG-CTT-3′) of the human IR. PCR amplification was carried out for 30 cycles of 20 s at 96 °C, 30 s at 58 °C, and 1.5 min at 72 °C using a DNA thermal cycler (PerkinElmer Life Sciences). After electrophoresis of the PCR products, the 600- and 636-bp DNA fragments representing the Ex11⁻ and Ex11⁺ IR isoforms were analyzed by scanning densitometry and compared with the standards. Standard preparation was carried out using mRNA from NIH/3T3 cells transfected with both IR isoform cDNAs mixed at various ratios and co-amplified by RT-PCR. To verify that the larger cDNA was really IR-B, RT-PCR products were subjected to *Ban*I digestion. Only cDNA containing exon 11, the restriction site for the enzyme, was digested.

Migration Assays

Cell migration assays were performed as previously described (40, 41) with minor modifications using modified Boyden chambers (6.5-mm diameter, 10-µm thickness, 8-µm pores; Transwell, Costar Corp., Cambridge, MA) containing polycarbonate membranes coated with 10 µg/ml collagen type IV. 36 h after transfection, HepG2 cells were serum-starved for 12 h. Cells were then removed from the plates with Hanks' balanced salt solution containing 5 mM EDTA, 25 mM HEPES (pH 7.2), and 0.01% trypsin; resuspended at 10^6 cells/ml; and added to the top of each migration chamber. Cells were allowed to migrate to the underside of the top chamber for 6 h in the presence or absence of 10 nM insulin, IGF-I, or IGF-II, which had been added to the lower chamber. Filters containing migrated and non-migrated cells were incubated with X-gal (Promega) as substrate according to the manufacturer's recommendations. Total cells stained with X-gal were scored using a ×40 objective. The non-migrated cells on the upper membrane surface were removed with a cotton swab, and the migrated cells attached to the bottom surface of the membrane stained with X-gal were counted as described above. Cell migration was expressed as the percent of migrated cells over total cells. Each determination was performed in triplicate.

BrdUrd Incorporation

HepG2 cells were seeded onto coverslips in six-well plates in complete medium. 24 h later, they were transfected with empty vector-IR-A/IR-B + histone H2B-GFP in triplicates as described above. 12 h later, the medium was replaced with Dulbecco's modified Eagle's medium and 0.1% BSA, and the cells were serum-starved for 24 h. Then, 10 nM insulin, IGF-I, or IGF-II was added, and the cells were further incubated for 36 h. Cells were incubated with 10 µM BrdUrd for 1 h, fixed in 3.7% paraformaldehyde in PBS for 15 min at room temperature, and incubated with 50 nM NH₄Cl in PBS. Cells were then permeabilized with 0.3% Triton X-100 in PBS; incubated with blocking solution containing 10% normal goat serum in PBS for 45 min at room temperature; and exposed to a mixture containing anti-BrdUrd antibody (diluted 1:200 in PBS plus 10% normal goat serum), 20 mM MgCl₂, 0.5% Nonidet P-40, and DNase I (1:500) for 1 h at room temperature. Coverslips were washed three times with PBS and incubated with Texas Red-conjugated goat anti-mouse antibody (1:200) in PBS plus 10% normal goat serum for 45 min at room temperature. Cells were counterstained with Hoechst 33258, and coverslips were mounted onto glass slides with gel/

mount (Biomeda). Coverslips were scored at ×40 magnification under an Olympus microscope, and images were randomly acquired with an ORCA digital camera (Hamamatsu) and superimposed with ImagePro-Plus software. Numbers were calculated as the percent of BrdUrd-incorporating cells among GFP-positive cells, and the increases induced by growth factors were calculated as the percent over basal levels.

RESULTS

IR-A and IR-B Moieties Can Form Hybrid-Rs with the Same Efficiency

Transfected R^- Cells—R^- cells, which do not express endogenous IGF-IR and have low levels of endogenous IR (which are not recognized by the anti-human IR antibodies used), were first transfected with a plasmid containing the cDNA of the human IGF-IR and then with a plasmid containing either the IR-A or IR-B cDNA. The stable transfectants obtained were evaluated for IR, IGF-IR, and Hybrid-R content, as described under "Experimental Procedures." In these cotransfected cell clones (IGF-IR + IR-A or IGF-IR + IR-B), Hybrid-R content was in close accordance with the value predicted by the random assembly model, indicating that each of the two IR isoforms can form Hybrid-Rs with the same efficiency (Table II). Western blot analyses, carried out as described under "Experimental Procedures," proved to be specific for each receptor measured (Fig. 1*A*) and confirmed ELISA data (Fig. 1*B* and Table II).

Established Human Cell Lines—To study native Hybrid-R functional characteristics in non-transfected cells, we studied a panel of established human cell lines (IM-9 lymphoblasts, ARO thyroid cancer cells, MDA-MB157 breast cancer cells, PC-3 prostate cancer cells, A549 lung cancer cells, and HepG2 hepatoblastoma cells). In these cells, we measured the IR isoform relative abundance and the IR, IGF-IR, and Hybrid-R content. With the exception of IM-9 cells, which expressed only IR-A, the remaining cell lines expressed both IR-A and IR-B. In these cell lines, IR-A content ranged from 24 to 82% of the total IR content. All these cells also expressed IGF-IRs and Hybrid-Rs. Hybrid-R content was in all cases in accordance with the random assembly model (Table II), confirming data obtained in transfected cells.

We also evaluated Hybrid-R content in HepG2 hepatoblastoma cells before and after exposure to dexamethasone, which causes cell differentiation and a change in the IR isoform relative abundance (29). In agreement with previous reports, IR-A decreased from 82 to 14% of the total cell IR content after dexamethasone-induced differentiation (Fig. 2 and Table III). Undifferentiated HepG2 cells therefore predominantly expressed Hybrid-Rs[A], whereas differentiated HepG2 cells predominantly expressed Hybrid-Rs[B].
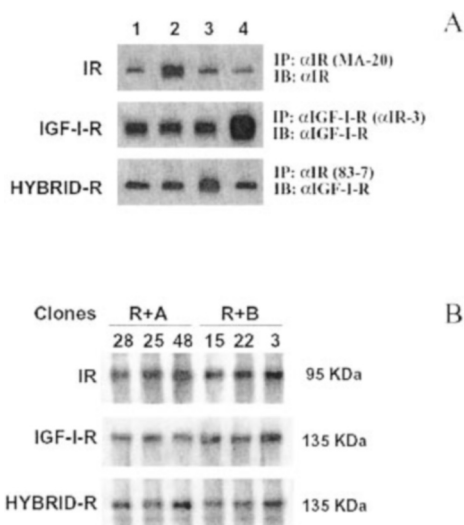
FIG. 1. *A*, specificity of Western blot analysis. To cell lysates from transfected fibroblast cell clones containing the IR (*upper panel*), the IGF-IR (*middle panel*), or the Hybrid-R (*lower panel*) were added 200 ng of purified IR (*lane 2*), Hybrid-R (*lane 3*), or IGF-IR (*lane 4*). In measurements of each receptor, no interference by the other two related receptors was observed. *B*, expression of the IR, IGF-IR, and Hybrid-R in stably transfected R⁻ cell clones. R⁻ cells were transfected either with IGF-IR and IR-A cDNAs (clones R⁺A28, R⁺A25, and R⁺A48) or with IGF-IR and IR-B cDNAs (clones R⁺B15, R⁺B22, and R⁺B3). Receptors were immunoprecipitated (*IP*) and detected by Western blot analysis as described under "Experimental Procedures." Clones R⁺A25 and R⁺B22 had a similar receptor content and were selected for functional studies. *IB*, immunoblot.
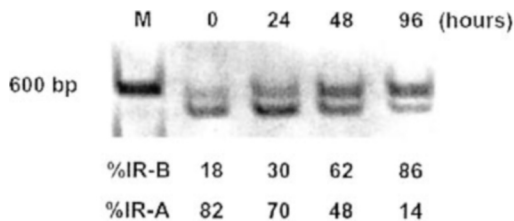

FIG. 2. **Time course of IR isoform expression in HepG2 cells during differentiation.** HepG2 cells were cultured in the absence (time 0) or in the presence of dexamethasone for the indicated times, and IR isoform expression was measured by RT-PCR. *Numbers* on the bottom indicate the relative abundance of IR isoform expression (%) calculated from densitometric analysis. The results are representative of three separate experiments. *M*, MARKER 600 bp.

Hybrid-Rs^A and Hybrid-Rs^B Have Different Binding and Activation Properties with Regard to Insulin and IGFs

To study the different binding characteristics of Hybrid-Rs^A and Hybrid-Rs^B, we used two double-transfected cell clones (R⁺A25 and R⁺B22) expressing similar amounts of either Hybrid-Rs^A or Hybrid-Rs^B (Fig. 1 and Table II). Cells were solubilized, and Hybrid-Rs were immunopurified with monoclonal antibody 83-7, which does not recognize the IGF-IR. ¹²⁵I-Labeled IGF-I was then allowed to bind to immunocaptured receptors in the absence or presence of increasing concentrations of various unlabeled ligands (insulin, IGF-I, and IGF-II).

The displacement curves indicate that Hybrid-Rs^A bound IGF-I with high affinity, ~8-fold higher compared with Hybrid-Rs^B (Fig. 3). Moreover, Hybrid-Rs^A also bound insulin and IGF-II with an affinity ~30-fold higher than that of Hybrid-Rs^B. In contrast, Hybrid-Rs^B bound only IGF-I with high affinity (Fig. 3). Half-maximal inhibition of ¹²⁵I-labeled IGF-I (EC₅₀) by the three ligands in both Hybrid-Rs^A and Hybrid-Rs^B is given in Table IV.

To compare the ligand affinity of Hybrid-Rs with that of homodimeric receptors, R⁻ cells were stably transfected with

cDNAs for IGF-IR, IR-A, or IR-B. Binding studies were carried out on immunopurified receptors from these cells by displacing either ¹²⁵I-labeled IGF-I or ¹²⁵I-labeled insulin with increasing concentrations of unlabeled ligands (insulin, IGF-I, and IGF-II). As previously reported (26), the IGF-IR bound both IGFs (but not insulin) with high affinity, and both IR isoforms bound insulin with high affinity and IGF-I poorly. However, only IR-A bound IGF-II with high affinity. EC₅₀ values are given in Table IV.

Data consistent with those obtained in stable transfectants of R⁻ cells were also obtained in Hybrid-Rs immunopurified from HepG2 cells (Fig. 3). In undifferentiated HepG2 cells (which predominantly express IR-A and Hybrid-Rs^A), IGF-I, IGF-II, or insulin displaced ¹²⁵I-labeled IGF-I with an affinity in the physiological concentration range (EC₅₀ = 0.4, 0.6, and 4.5 nM, respectively). In contrast, in differentiated HepG2 cells (which predominantly express IR-B and Hybrid-Rs^B), the EC₅₀ values were 1.8 for IGF-I, 4.0 for IGF-II, and 20 nM for insulin (Fig. 3).

The binding characteristics of Hybrid-Rs were also studied in a variety of established human cell lines (Table II). In Hybrid-Rs immunopurified from IM-9 cells (which express only IR-A and Hybrid-Rs^A) or from PC-3, MDA-MB157, and ARO cells (all which predominantly express Hybrid-Rs^A), both IGFs and insulin efficiently displaced ¹²⁵I-labeled IGF-I. EC₅₀ values ranged 0.2 to 0.6 nM for IGF-I, 0.3 to 0.7 nM for IGF-II, and 1.8 to 3.2 nM for insulin. In contrast, in A549 cells (which predominantly express IR-B (76%) and Hybrid-Rs^B), the EC₅₀ values were 1.5 nM for IGF-I, 10 nM for IGF-II, and >100 nM for insulin.

Receptor autophosphorylation was evaluated in intact cells expressing either only Hybrid-Rs^A or Hybrid-Rs^B after exposure to either insulin or IGFs in the presence of a molar excess of the IR-blocking antibody MA-10, which does not recognizes Hybrid-Rs, as evaluated by immunoprecipitation experiments (data not shown). This procedure was used to avoid the interference of IRs. Cells were then solubilized, and receptors were immunopurified with antibody 83-7 (which recognizes the IR and Hybrid-R, but not the IGF-IR). Autophosphorylation/activation of immunopurified Hybrid-Rs was measured by Western blotting. As shown in Fig. 4*A*, IGF-I, IGF-II, and insulin were all able to efficiently activate Hybrid-Rs^A, whereas only IGF-I was able to efficiently activate Hybrid-Rs^B. Both IGF-II and insulin were much less effective in Hybrid-Rs^B than in Hybrid-Rs^A. Similar results were obtained in parallel experiments in which Hybrid-R autophosphorylation was quantitated by ELISA (Fig. 4*B*). These autophosphorylation data are therefore in close accordance with results from binding studies and suggest that Hybrid-Rs^A may be regarded as additional receptors for IGF-I, IGF-II, and also insulin, whereas, in contrast, Hybrid-Rs^B should be regarded as selective receptors for IGF-I.

Hybrid-Rs^A (but Not Hybrid-Rs^B) Shift Insulin to IGF-IR Signaling

Because insulin bound to the Hybrid-R^A with an affinity within the physiological range, we evaluated the ability of insulin to activate the IGF-IR β-subunit of the Hybrid-R^A. For this purpose, either R⁺A25 or R⁺B22 cell clones were stimulated with insulin, IGF-I, or IGF-II and then solubilized as described under "Experimental Procedures." Samples were immunoprecipitated with anti-phosphotyrosine antibody 4G10, subjected to SDS-PAGE, and blotted with anti-IGF-IR antibody. In R⁺A25 cells, which express only Hybrid-Rs^A, insulin recruited the IGF-IR to the tyrosine phosphorylation cascade with a potency similar to that of IGF-II, albeit lower than that of IGF-I (Fig. 5). By contrast, in R⁺B22 cells, which express

TABLE III

IR-A relative abundance and IR, IGF-IR, and Hybrid-R content in a panel of human malignant cells and in human hepatoma HepG2 cells before and after differentiation

Cells	IR-A	IR[a]	IGF-IR[a]	Hybrid-R[a]	
				Measured	Predicted
	%				
IM-9	100	12.0 ± 0.6	26.0 ± 4.4	30.0 ± 4.2	35.3
ARO	80	8.0 ± 0.9	10.8 ± 1.0	25.5 ± 3.4	18.6
MDA-MB157	70	11.0 ± 0.87	2.0 ± 0.5	12.0 ± 2.2	9.4
PC-3	68	8.5 ± 2.2	0.9 ± 0.1	9.5 ± 3.1	5.5
A549	24	0.18 ± 0.03	17.0 ± 4.2	2.5 ± 0.1	3.5
HepG2					
Undifferentiated	82	3.4 ± 0.8	2.1 ± 0.4	6.5 ± 0.4	5.3
Differentiated	14	8.2 ± 0.6	3.2 ± 0.9	10.6 ± 0.2	10.2

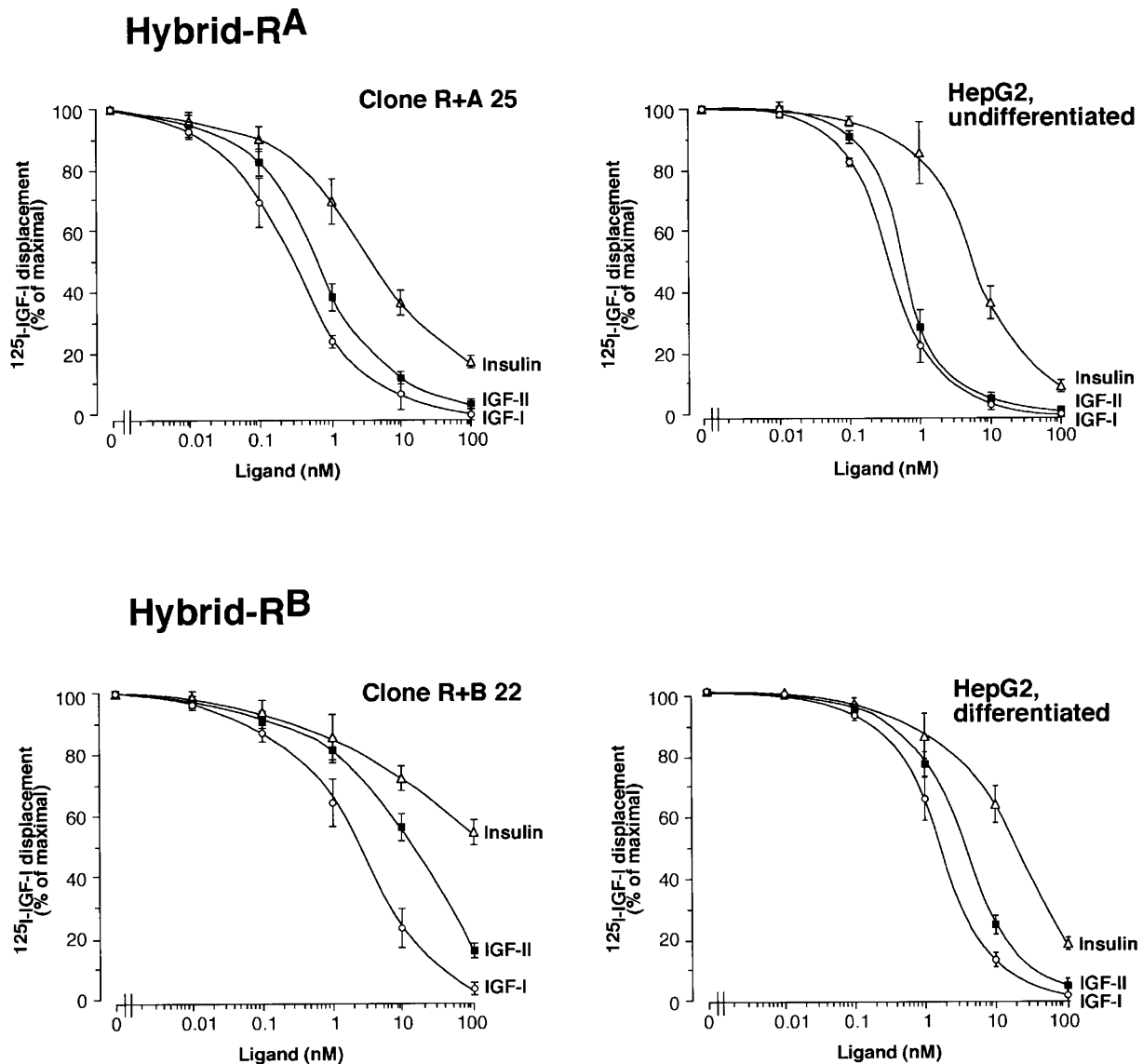[a] Receptor content expressed as ng/100 μg of protein.

FIG. 3. **Competition inhibition curves of ^{125}I-labeled IGF-I binding to immunopurified Hybrid-Rs[B] or Hybrid-Rs[A].** Immunopurified Hybrid-Rs[A] or Hybrid-Rs[B] were incubated with ^{125}I-labeled IGF-I (10 pM) in the absence or presence of increasing concentrations of insulin, IGF-I, or IGF-II as described under "Experimental Procedures." The data represent means $\pm$ S.E. of three separate experiments run in triplicate. Hybrid-Rs[A] were immunopurified either from R^{-} cells transfected with both IR-A and IGF-IR (clone R[+]A25) or from undifferentiated HepG2 cells. Hybrid-Rs[B] were immunopurified either from R^{-} cells transfected with both IR-B and IGF-IR (clone R[+] B22) or from differentiated HepG2 cells.

only Hybrid-Rs[B], IGF-IR recruitment by insulin was very weak and much lower than that induced by IGF-I or IGF-II (Fig. 5). Reblotting with anti-phosphotyrosine antibody 4G10 showed that, in R[+]A25 cells, IGF-II stimulated the tyrosine phosphorylation of the 97-kDa band (containing both the IR and IGF-IR

β-subunits) with a higher potency than in R[+]B22 cells.

We then evaluated whether insulin, via the Hybrid-R[A], is able to activate IGF-IR-specific intracellular mediators like the small adapter protein CrkII, which is phosphorylated by the IGF-IR, but not by the IR (9, 42, 43). To this purpose, either

IR Isoforms Affect Insulin/IGF-I Hybrid Receptor Properties

TABLE IV
Binding affinity of insulin, IGF-I, and IGF-II for immunopurified receptors (Hybrid-R[A], Hybrid-R[B], IGF-IR, IR-A, and IR-B from transfected R^{−} cells

R^{−} cells	EC$_{50}$ of unlabeled ligand		
	Insulin	IGF-I	IGF-II
	nM		
Hybrid-R[A]	3.7 ± 0.9	0.3 ± 0.2	0.6 ± 0.1
Hybrid-R[B]	>100	2.5 ± 0.5	15.0 ± 0.9
IGF-IR	>30.0	0.2 ± 0.3	0.6 ± 1.0
IR-A	0.2 ± 0.2	>30.0	0.9 ± 0.4
IR-B	0.3 ± 0.4	>30.0	11.0 ± 5.0

R[+]A25 or R[+]B22 cell clones were stimulated with insulin or IGF-I, and immunopurified receptors were incubated with CrkII and ATP in kinase buffer as described under "Experimental Procedures." When IRs were immunopurified (with antibody MA-20), no CrkII phosphorylation was observed (Fig. 6), confirming that CrkII is not a substrate of the IR. In contrast, when Hybrid-Rs were immunopurified (with antibody 83-7), Hybrid-Rs[A] (but not Hybrid-Rs[B]) were able to phosphorylate CrkII in response to insulin (Fig. 6), a difference that may be explained by the high affinity of insulin for Hybrid-Rs[A]. Both Hybrid-Rs[A] and Hybrid-Rs[B] were able to phosphorylate CrkII in response to IGF-I. Taken together, these data suggest that insulin may activate IGF-IR-specific intracellular pathways by interacting with Hybrid-Rs[A].

Hybrid-R[A] and Hybrid-R[B] Post-receptor Signaling

Double-transfected R[+]A25 and R[+]B22 cell clones were used to study the ligand ability to activate the post-receptor signaling pathways in intact cells expressing similar amounts of the three receptor subtypes (IGF-IR, IR, and Hybrid-R), but different isoforms. Parallel experiments were also carried out in cells containing only IR-A (R[−]IR-A cells), IR-B (R[−]IR-B cells), or IGF-IR (R^{+} cells). Cells were exposed to each ligand (10 nM) for 10 min, and phosphorylation of the intracellular substrates ERK1/2 kinase (p42/p44 mitogen-activated protein kinase) and Akt was subsequently measured by Western blotting.

Both substrates ERK1/2 and Akt had similar activation patterns in response to the different ligands. Insulin was the most potent stimulating factor in both double-transfected cell clones, as expected by the presence of elevated IR levels (Fig. 7). IGF-II was approximately as potent as IGF-I in R[+]A25 cells (Fig. 7) because of its high affinity for both IR-A and Hybrid-Rs[A], whereas it was less potent than IGF-I in R[+]B22 cells (Fig. 7), in accordance with data obtained from the anti-phosphotyrosine antibody blot in Fig. 5. These data confirm that IR-A predominance enhances the cell sensitivity to IGF-II (which can bind to IGF-IRs, IR-A, and Hybrid-Rs[A]). Similar results were obtained in HepG2 cells: undifferentiated cells (mostly expressing Hybrid-Rs[A]) behaved similarly to R[+]A25 cells, whereas differentiated cells (mostly expressing Hybrid-Rs[B]) behaved similarly to R[+]B22 cells (data not shown).

In cell clones containing only IR-A, both insulin and IGF-II stimulated Akt and ERK1/2 phosphorylation to a similar extent (Fig. 8). In contrast, in cell clones containing only IR-B, insulin (but not IGFs) was able to stimulate Akt and ERK1/2 phosphorylation. In R^{+} cells (which express only the IGF-IR), the two IGFs were roughly equally potent in stimulating Akt and ERK1/2 phosphorylation, whereas insulin was not very effective (Fig. 8).

Biological Effects of Either Insulin or IGFs in Cells Predominantly Expressing Either Hybrid-Rs[A] or Hybrid-Rs[B]

We evaluated whether the presence of Hybrid-Rs[A] or Hybrid-Rs[B] may affect cell biological responses (such as cell prolifera-

tion and migration) to either insulin or IGFs. To avoid possible proliferation and migration differences due to the differentiation state, undifferentiated HepG2 cells were forced to overexpress either Hybrid-Rs[A] or Hybrid-Rs[B] by transient IR-A or IR-B cDNA transfection. Control cells were obtained by transfection of an empty vector. Transfection efficiency, evaluated by histone H2B-GFP and β-galactosidase, ranged from 15 to 20% (Fig. 9A).

Cell proliferation was measured by scoring BrdUrd-labeled nuclei in GFP-positive cells. Both IR-A and IR-B transfection enhanced cell proliferation in response to insulin as compared with empty vector transfection. By contrast, only IR-A transfection significantly enhanced cell proliferation in response to both IGFs. IR-B transfection only slightly enhanced proliferation in response to IGF-I and was totally ineffective for IGF-II-stimulated cell proliferation (Fig. 9B).

We also measured cell migration by scoring β-galactosidase-positive cells that migrated to the lower side of Transwells (Fig. 10A). IR-A transfection significantly enhanced cell migration in response to all three ligands as compared with empty vector transfection. In contrast, IR-B transfection only slightly enhanced cell migration in response to IGF-I, but not in response to insulin or IGF-II (Fig. 10B).

Taken together, these data suggest that the relative abundance of IR isoforms differentially regulates two major biological effects (such as cell proliferation and migration) in response to both insulin and IGFs. IR-A overexpression and subsequent Hybrid-R[A] formation markedly enhance cell biological responses to both IGFs, whereas IR-B overexpression does not. In addition, whereas cell proliferation in response to insulin is activated via both IR-A and IR-B, only IR-A increases cell migration in response to insulin, an effect most likely mediated by the activation of the IGF signaling pathway, via insulin binding to the Hybrid-R[A].

DISCUSSION

The main finding of our study is that the differential expression of the two isoforms of the human IR constitutes a molecular switch for the preferential activation of either the IR or IGF-I pathway. This is determined by both binding and signaling specificities of the two Hybrid-R types that are formed. In particular, predominant IR-A expression in cells coexpressing the IGF-IR leads to increased formation of Hybrid-Rs[A], which up-regulates the IGF system by two different mechanisms: (*a*) binding and activation with high affinity by both IGF-I and IGF-II (which do not occur with the Hybrid-R[B]) and (*b*) activation of the IGF-IR pathway also after insulin binding.

In contrast, predominant IR-B expression leads to high binding specificity whereby insulin activates only its own receptor and post-receptor signaling. Moreover, IR-B will sequestrate part of the IGF-IR moieties to form Hybrid-Rs[B], which have a reduced affinity for IGF-I and especially for IGF-II. This combined effect will result in reduced IGF system activity.

Although IR isoforms and insulin/IGF-I hybrid receptors have been extensively studied (18, 19, 22–25, 29), their biological role was unclear. Hybrid-Rs are present in cells and tissues coexpressing both IRs and IGF-IRs and are often the most abundant receptor subtype (14, 16, 17).

Functional studies have consistently shown that Hybrid-Rs behave similarly to homotypic IGF-IRs rather than to homotypic IRs (14–19, 22, 23). Using immunopurified receptors, Soos *et al.* (22) have shown that Hybrid-Rs bind IGF-I with high affinity, similar to typical IGF-IRs, whereas they bind insulin with much lower affinity (~20-fold lower compared with IRs). Moreover, insulin does not effectively displace Hybrid-R-bound IGF-I, possibly because IGF-I interaction with the α-subunit of the IGF-IR allosterically inhibits insulin bind-
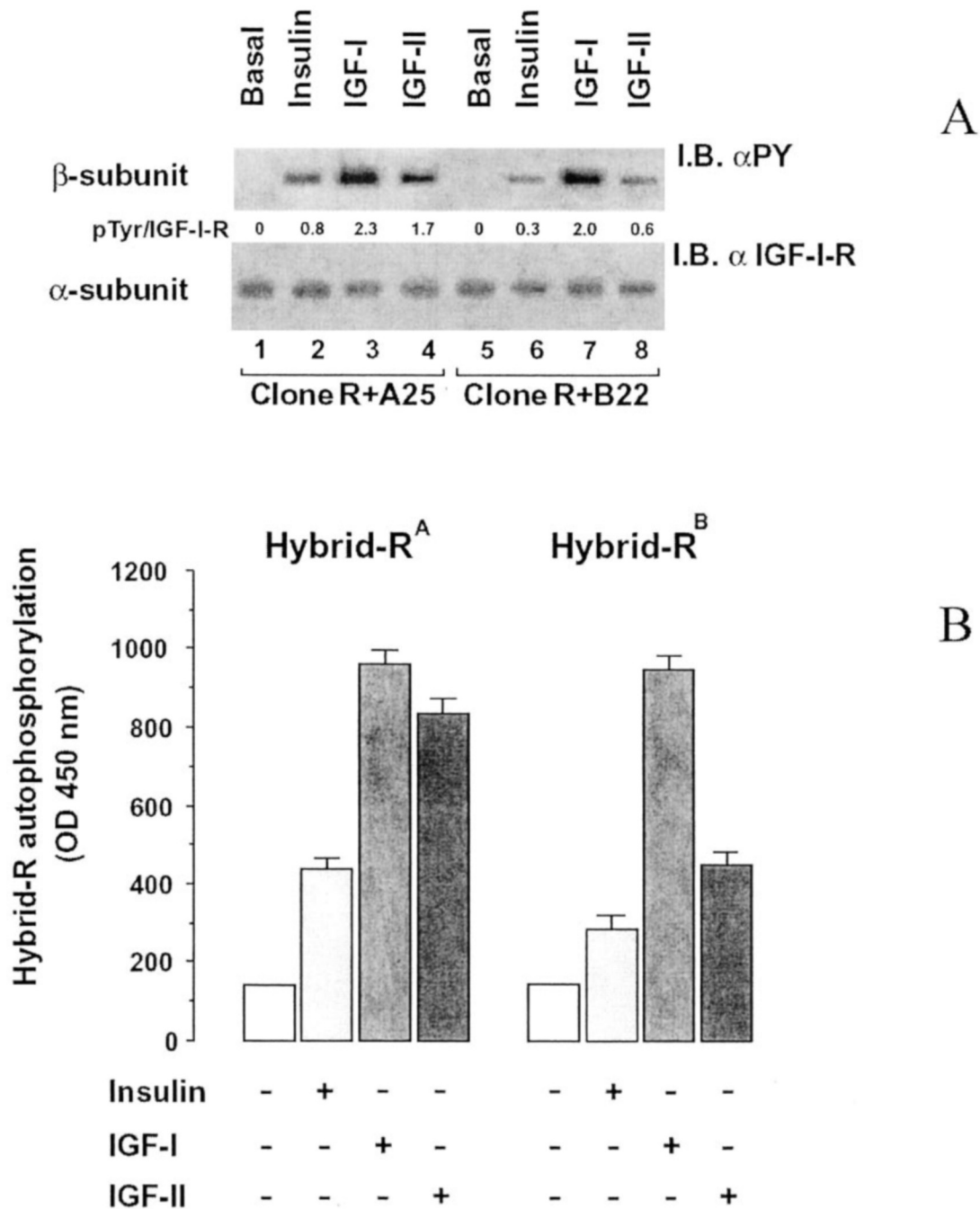
FIG. 4. **Autophosphorylation of Hybrid-Rs^A and Hybrid-Rs^B in response to insulin, IGF-I, and IGF-II.** Cultured cells containing either Hybrid-Rs^A (clone R$^+$A25) or Hybrid-Rs^B (clone R$^+$B22) were exposed to insulin, IGF-I, or IGF-II (10 nM) in the presence of the IR-blocking antibody MA-10. Cells were then solubilized, and Hybrid-Rs were immunopurified with antibody 83-7. *A*, Western blot analysis. *Upper panel*, anti-phosphotyrosine (*αPY*) antibody immunoblot (*I.B.*). *Numbers* on the bottom indicate means ± S.D. of the densitometric reading of three independent experiments (arbitrary units). *Lower panel*, reblotting with anti-IGF-IR antibody. A representative experiment is shown. *B*, ELISA. Receptor autophosphorylation in response to ligands was measured by ELISA as described under "Experimental Procedures." The data represent means ± S.E. of three separate experiments.

ing (23). According to these observations, Hybrid-Rs are auto-phosphorylated more efficiently after binding IGF-I compared with insulin (22).

As Hybrid-Rs are believed to result from random assembly of insulin and IGF-I half-receptors (17), their cell content is directly related to the expression level of the two receptors. Therefore, in cells expressing high IR levels, Hybrid-R content may exceed typical IR and IGF-IR content (18, 19). This will shift the major ligand binding from insulin to IGFs and may have relevant biological consequences in both metabolic disorders and cancer. For instance, increased Hybrid-R formation

has been suggested to reduce the availability of typical IRs, thus contributing to insulin resistance in diabetes (44–46); however, these data are controversial. Interestingly, certain human cancers (namely thyroid and breast cancers) (18–21, 28, 47) have been shown to overexpress IRs and, as a consequence, to express very high levels of Hybrid-Rs. In these models, Hybrid-Rs were able to mediate cancer cell growth in response to IGF-I, suggesting that they may provide a selective growth advantage to malignant cells (18, 19).

No previous study has addressed the functional characteristics of the Hybrid-R with relation to the IR isoform involved.
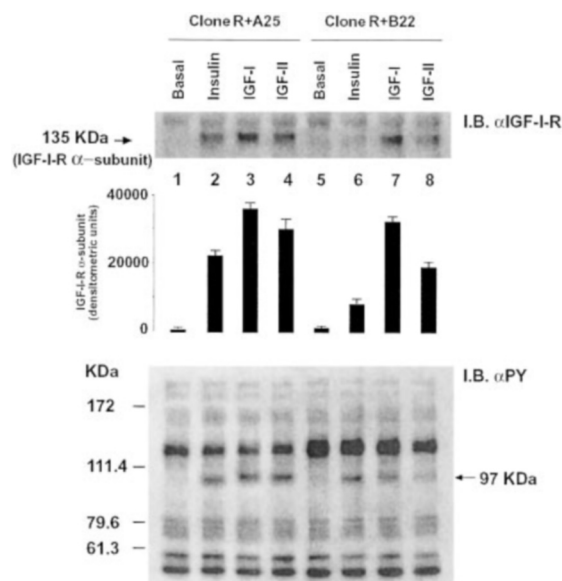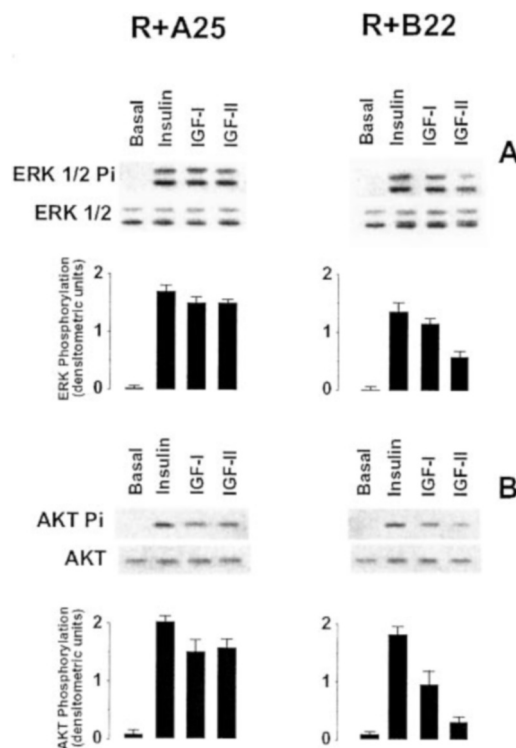
FIG. 5. **Involvement of the IGF-IR moiety in Hybrid-R^A and Hybrid-R^B activation.** R$^+$A25 and R$^+$B22 cells were treated with the indicated ligands (10 nM), and tyrosine-phosphorylated proteins were immunoprecipitated as indicated under "Experimental Procedures." *Upper panel*, immunoblot (*I.B.*) with anti-IGF-IR antibody. A representative experiment is shown. *Middle panel*, densitometric data representing means ± S.E. of three separate experiments. *Lower panel*, reblotting with anti-phosphotyrosine (α*PY*) antibody.
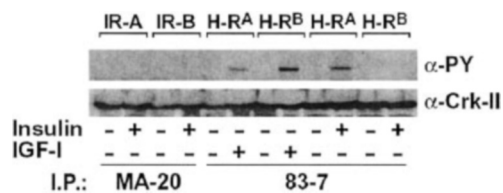
FIG. 6. *In vitro* **tyrosine kinase activity of the IR and Hybrid-R for CrkII.** R$^+$A25 and R$^+$B22 cells were stimulated *in vivo* with the indicated ligands. The tyrosine kinase activity of immunoprecipitated (*I.P.*) receptors for CrkII was determined *in vitro* as indicated under "Experimental Procedures." *Upper panel*, anti-phosphotyrosine (α*PY*) blot; *lower panel*, anti-Crk antibody reblotting. A representative experiment is shown. *H-R*, Hybrid-R.

FIG. 7. **ERK1/2 and Akt activation by insulin, IGF-I, and IGF-II in transfected R$^-$ fibroblasts expressing either Hybrid-Rs^A or Hybrid-Rs^B.** Serum-starved R$^+$A25 and R$^+$B22 cells were exposed to 10 nM insulin, IGF-I, or IGF-II. *A*, ERK1/2 activation. *Upper panel*, anti-phospho-ERK antibody blot showing results representative of three separate experiments; *middle panel*, reblotting with anti-ERK antibody; *lower panel*, densitometric reading (phospho-ERK/total ERK) representing means ± S.E. of three separate experiments. *B*, Akt activation. *Upper panel*, anti-phospho-Akt antibody blot showing results representative of three separate experiments; *middle panel*, reblotting with anti-Akt antibody; *lower panel*, densitometric reading (phospho-Akt/total Akt) representing means ± S.E. of three separate experiments.

Although the precise role of the two IR isoforms is not entirely clear, this issue has become relevant following recent evidence that the relative abundance of IR isoforms is tightly regulated by tissue-specific factors, stage of development, and cell differentiation (24, 25, 29). IR-A is the predominant isoform in fetal tissues; binds IGF-II with high affinity (26); and mediates fetal growth in response to IGF-II, as also suggested by genetic studies carried out in transgenic mice (48, 49). Moreover, when cells transform and become malignant, dedifferentiation is often associated with an increased IR-A relative abundance, providing a selective growth advantage to malignant cells via an autocrine or paracrine loop with locally produced IGF-II (27, 28). IR-B is the predominant IR isoform in normal adult tissues that are major target tissues for the metabolic effects of insulin (adipose tissue, liver, and muscle) (24, 25).

In this study, we have demonstrated that each IR isoform affects Hybrid-R biology by using three different models: transfected R$^-$ mouse fibroblasts, undifferentiated and differentiated HepG2 human hepatoblastoma cells, and a panel of human cell lines with different relative abundance of the two IR isoforms. R$^-$ mouse fibroblasts were transfected to coexpress the IGF-IR and either IR-A or IR-B to obtain cells containing

only either the Hybrid-R^A or Hybrid-R^B. HepG2 cells provide a natural model expressing up to 80% IR-A of the total IR content under basal conditions (undifferentiated state), but only ~15% after differentiation with dexamethasone. In these models, we found that the two IR isoforms have a similar ability to form hybrids with the IGF-IR because Hybrid-R content, measured by a specific ELISA, was very close to the value predicted according to the random assembly model on the basis of the cell content of IRs and IGF-IRs.

We first studied ligand binding and observed that the two Hybrid-R types bind ligands with different affinity. Immunopurified Hybrid-Rs^B have a high affinity for IGF-I (ED$_{50}$ = 2.5 nM IGF-I), bind IGF-II with 6-fold lower affinity, and do not appreciably bind insulin. Accordingly, Hybrid-Rs^B are activated by IGF-I and to a lesser extent by IGF-II and are not by insulin. In contrast, immunopurified Hybrid-Rs^A have a higher affinity for IGF-I (ED$_{50}$ = 0.3 nM IGF-I) compared with Hybrid-Rs^B and bind IGF-II with a similar affinity (ED$_{50}$ = 0.6 nM IGF-II) and insulin with a lower affinity (ED$_{50}$ = 3.7 nM insulin), but still in the physiological range. In agreement with binding data, Hybrid-Rs^A can be activated by both IGFs and also by insulin.

We then studied post-receptor signaling and, more specifically, whether insulin can induce IGF-IR β-subunit phosphorylation in intact cells expressing Hybrid-Rs. As expected from the binding data, exposure to insulin caused IGF-IR β-subunit phosphorylation in cells expressing Hybrid-Rs^A, but not in cells

FIG. 8. **ERK1/2 and Akt activation by insulin, IGF-I, and IGF-II in transfected R⁻ fibroblasts expressing only IR-A(R⁻IR-A) or IR-B(R⁻IR-B and in R⁺ fibroblasts expressing only IGF-IRs (R⁺).** Serum-starved cells were exposed to 10 nM insulin, IGF-I, or IGF-II. *A*, ERK1/2 activation. *Upper panel*, anti-phospho-ERK antibody blot showing results representative of three separate experiments; *middle panel*, reblotting with anti-ERK antibody; *lower panel*, densitometric reading (phospho-ERK/total ERK) representing means ± S.E. of three separate experiments. *B*, Akt activation. *Upper panel*, anti-phospho-Akt antibody blot showing results representative of three separate experiments; *middle panel*, reblotting with anti-Akt antibody; *lower panel*, densitometric reading (phospho-Akt/total Akt) representing means ± S.E. of three separate experiments.
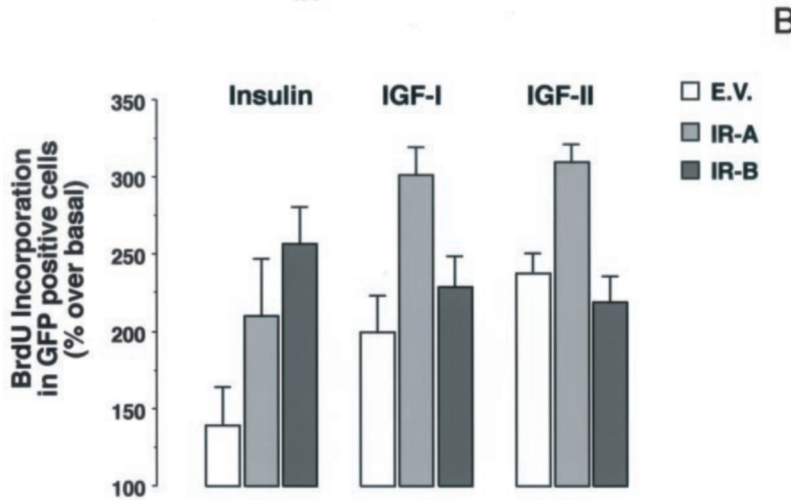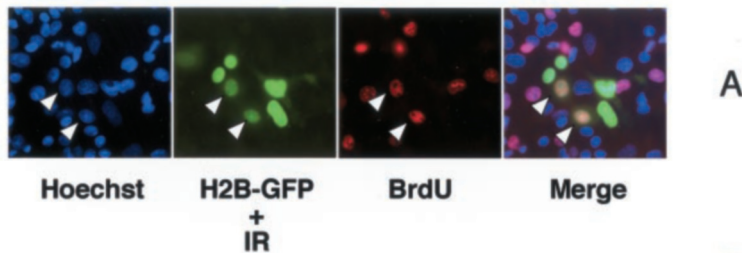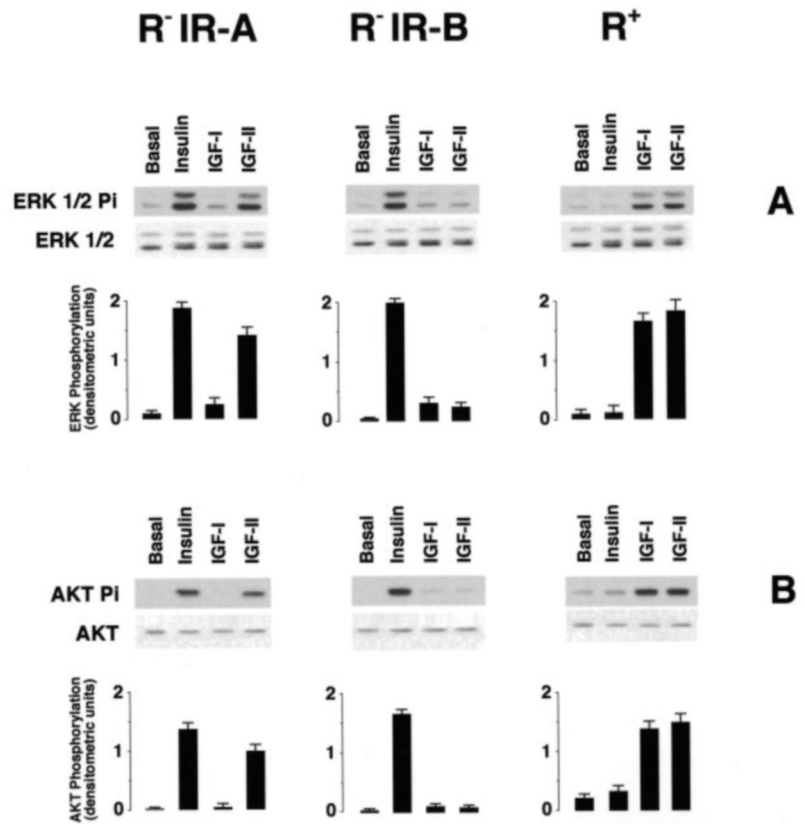
FIG. 9. **Proliferation in HepG2 cells transfected with either IR-A or IR-B cDNA in response to insulin, IGF-I, or IGF-II.** *A*, proliferation was measured by scoring BrdUrd (*BrdU*) incorporation in GFP-positive cells under an immunofluorescence microscope. *B*, *bars* indicate cell proliferation over basal levels in response to insulin, IGF-I, or IGF-II in cells transfected with an empty vector (*E.V.*) or IR-A or IR-B cDNA. Values are means ± S.D. of three experiments performed in triplicate and were calculated as described under "Experimental Procedures."

expressing Hybrid-Rs[B]. Although the β-subunits of the IR and IGF-IR share >80% homology, differences exist in the recruitment of intracellular mediators and the biological effects elicited by the two receptors: more pronounced metabolic effects follow activation of the IR, whereas more pronounced mitogenic, anti-apoptotic, and transforming effects follow activation of the IGF-IR (1–13). These differences in biological effects

(6–13) are the consequence of the different activation of intracellular mediators. CrkII is an adapter protein consisting primarily of SH2 and SH3 domains; is a specific substrate of the IGF-IR (9, 42, 43); and mediates certain protein-protein interactions involved in signaling pathways that lead to cytoskeletal rearrangement, cell growth, differentiation, apoptosis, and transformation (41). We found here that CrkII is also a sub-
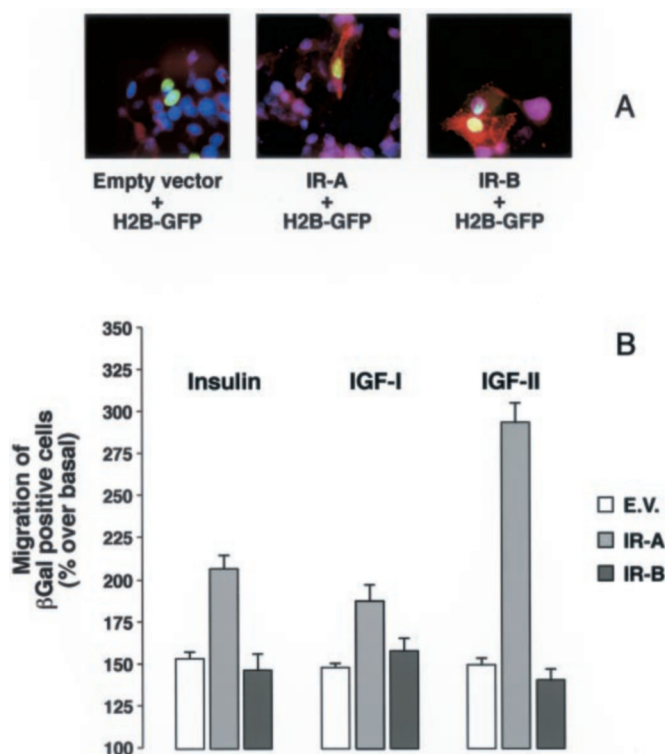
FIG. 10. **Chemotaxis of HepG2 cells transfected with either IR-A or IR-B cDNA in response to insulin, IGF-I, or IGF-II.** *A,* shown is the immunofluorescence staining of insulin receptors in HepG2 cells transiently transfected with either IR-A or IR-B cDNA. Paraformaldehyde-fixed cells were stained with anti-IR antibody 29B4, and images were acquired as described under "Experimental Procedures." *B,* transfected cells were allowed to migrate in Boyden chambers upon stimulation with 10 nM insulin, IGF-I, or IGF-II and stained for β-galactosidase activity as described under "Experimental Procedures." *Bars* indicate migration of β-galactosidase (βGal)-positive cells in response to insulin, IGF-I, or IGF-II in cells transfected with a β-galactosidase vector or cotransfected with IR-A or IR-B cDNA and a β-galactosidase vector. Values are means ± S.D. of three experiments performed in triplicate and were calculated as described under "Experimental Procedures." *E.V.*, empty vector.

strate for IGF-I-stimulated Hybrid-Rs. Moreover, CrkII is also phosphorylated after insulin stimulation of Hybrid-Rs[A] (but not Hybrid-Rs[B]), confirming that Hybrid-Rs[A] may shift typical insulin signaling to IGF-IR signaling.

This phenomenon may have biological relevance in hyperinsulinemic insulin-resistant states and in cancer. In hyperinsulinemic states, elevated insulin levels are suggested to cross-react with the IGF-IR. As insulin binds the Hybrid-R[A] with an affinity at least 10-fold higher compared with the IGF-IR, it is likely that the most activation of the IGF system by elevated insulin levels (50) occurs via the Hybrid-R[A] rather than the IGF-IR. Most cancer cells do preferentially express IR-A and consequently Hybrid-Rs[A]. In thyroid cancer, for instance, cell dedifferentiation is associated with both progressive IR-A prevalence and increased autocrine IGF-II production (28). These cancer cells therefore acquire a higher sensitivity not only to IGF-I, but also to IGF-II and insulin.

Finally, we observed that two major biological effects (such as proliferation and migration) are differentially regulated by the same factors depending on the prevalence of either Hybrid-Rs[A] or Hybrid-Rs[B]. In HepG2 cells, proliferation and migration in response to IGFs were greatly stimulated in cells overexpressing Hybrid-Rs[A], but not in cells expressing Hybrid-Rs[B]. Moreover, insulin stimulated cell migration only in cells overexpressing Hybrid-Rs[A], most likely via activation of IGF-IR β-subunit signaling pathways.

This study indicates for the first time that regulation of IR isoform expression has important implications in both insulin and IGF signaling. In cells predominantly expressing IR-A (and coexpressing the IGF-IR), the IGF-IR intracellular cascade may be activated in response to insulin and IGFs via Hybrid-R[A] activation. In contrast, in cells predominantly expressing IR-B (as most differentiated cells do), insulin will activate only the typical IR signaling pathway, whereas the response to IGFs will mainly occur via typical IGF-IRs because Hybrid-Rs[B] have a reduced affinity for IGFs and because insulin, at physiological concentrations, will not bind. A better understanding of the molecular mechanisms regulating the alternative splicing process of the IR gene will therefore provide important information for the regulation of cell metabolism and proliferation and other biological functions.

REFERENCES

1. Avruch, J. (1998) *Mol. Cell. Biochem.* **182,** 31–48
2. Roth, R. A., Steele-Perkins, G., Hari, J., Stover, C., Pierce, S., Turner, J., Edman, J. C., and Rutter, W. J. (1988) *Cold Spring Harbor Symp. Quant. Biol.* **53,** 537–543
3. White, M. F. (1998) *Mol. Cell. Biochem.* **182,** 3–11
4. Laviola, L., Giorgino, F., Chow, J. C., Baquero, J. A., Hansen, H., Ooi, J., Zhu, J., Riedel, H., and Smith, R. J. (1997) *J. Clin. Invest.* **99,** 830–837
5. Cheatham, B., and Kahn, C. R. (1995) *Endocr. Rev.* **16,** 117–142
6. Sasaoka, T., Ishiki, M., Sawa, T., Ishihara, H., Takata, Y., Imamura, T., Usui, I., Olefsky, J. M., and Kobayashi, M. (1996) *Endocrinology* **137,** 4427–4434
7. Nakae, J., Kido, Y., and Accili, D. (2001) *Endocr. Rev.* **22,** 818–835
8. Dupont, J., and LeRoith, D. (2001) *Horm. Res.* (*Basel*) **55,** Suppl. 2, 22–26
9. Koval, A. P., Blakesley, V. A., Roberts, C. T., Jr., Zick, Y., and LeRoith, D. (1998) *Biochem. J.* **330,** 923–932
10. Baserga, R. (1995) *Cancer Res.* **55,** 249–252
11. Prisco, M., Romano, G., Peruzzi, F., Valentinis, B., and Baserga, R. (1999) *Horm. Metab. Res.* **31,** 80–89
12. Kido, Y., Nakae, J., and Accili, D. (2001) *J. Clin. Endocrinol. Metab.* **86,** 972–979
13. De Meyts, P., Urso, B., Christoffersen, C. T., and Shymko, R. M. (1995) *Ann. N. Y. Acad. Sci.* **766,** 388–401
14. Soos, M. A., Whittaker, J., Lammers, R., Ullrich, A., and Siddle, K. (1990) *Biochem. J.* **270,** 383–390
15. Kasuya, J., Paz, I. B., Maddux, B. A., Goldfine, I. D., Hefta, S. A., and Fujita-Yamaguchi, Y. (1993) *Biochemistry* **32,** 13531–13536
16. Seely, B. L., Reichart, D. R., Takata, Y., Yip, C., and Olefsky, J. M. (1995) *Endocrinology* **136,** 1635–1641
17. Bailyes, E. M., Nave, B. T., Soos, M. A., Orr, S. R., Hayward, A. C., and Siddle, K. (1997) *Biochem. J.* **327,** 209–215
18. Pandini, G., Vigneri, R., Costantino, A., Frasca, F., Ippolito, A., Fujita-Yamaguchi, Y., Siddle, K., Goldfine, I. D., and Belfiore, A. (1999) *Clin. Cancer Res.* **5,** 1935–1944
19. Belfiore, A., Pandini, G., Vella, V., Squatrito, S., and Vigneri, R. (1999) *Biochimie* (*Paris*) **81,** 403–407
20. Papa, V., Pezzino, V., Costantino, A., Belfiore, A., Giuffrida, D., Frittitta, L., Vannelli, G. B., Brand, R., Goldfine, I. D., and Vigneri, R. (1990) *J. Clin. Invest.* **86,** 1503–1510
21. Papa, V., Gliozzo, B., Clark, G. M., McGuire, W. L., Moore, D., Fujita-Yamaguchi, Y., Vigneri, R., Goldfine, I. D., and Pezzino, V. (1993) *Cancer Res.* **53,** 3736–3740
22. Soos, M. A., Field, C. E., and Siddle, K. (1993) *Biochem. J.* **290,** 419–426
23. Frattali, A. L., and Pessin, J. E. (1993) *J. Biol. Chem.* **268,** 7393–7400
24. Moller, D. E., Yokota, A., Caro, J. F., and Flier, J. S. (1989) *Mol. Endocrinol.* **3,** 1263–1269
25. Mosthaf, L., Grako, K., Dull, T. J., Coussens, L., Ullrich, A., and McClain, D. A. (1990) *EMBO J.* **9,** 2409–2413
26. Frasca, F., Pandini, G., Scalia, P., Sciacca, L., Mineo, R., Costantino, A., Goldfine, I. D., Belfiore, A., and Vigneri, R. (1999) *Mol. Cell. Biol.* **19,** 3278–3288
27. Sciacca, L., Costantino, A., Pandini, G., Mineo, R., Frasca, F., Scalia, P., Sbraccia, P., Goldfine, I. D., Vigneri, R., and Belfiore, A. (1999) *Oncogene* **18,** 2471–2479
28. Vella, V., Sciacca, L., Pandini, G., Mineo, R., Squatrito, S., Vigneri, R., and Belfiore, A. (2001) *Mol. Pathol.* **54,** 121–124
29. Kosaki, A., and Webster, N. J. (1993) *J. Biol. Chem.* **268,** 21990–21996
30. Forsayeth, J. R., Montemurro, A., Maddux, B. A., DePirro, R., and Goldfine, I. D. (1987) *J. Biol. Chem.* **262,** 4134–4140
31. Roth, R. A., Cassell, D. J., Wong, K. Y., Maddux, B. A., and Goldfine, I. D. (1982) *Proc. Natl. Acad. Sci. U. S. A.* **79,** 7312–7316
32. Soos, M. A., Siddle, K., Baron, M. D., Heward, J. M., Luzio, J. P., Bellatin, J., and Lennox, E. S. (1986) *Biochem. J.* **235,** 199–208
33. Ganderton, R. H., Stanley, K. K., Field, C. E., Coghlan, M. P., Soos, M. A., and Siddle, K. (1992) *Biochem. J.* **288,** 195–205
34. Kull, F. C., Jr., Jacobs, S., Su, Y. F., Svoboda, M. E., Van Wyk, J. J., and

Cuatrecasas, P. (1983) *J. Biol. Chem.* **258,** 6561–6566

35. Soos, M. A., Field, C. E., Lammers, R., Ullrich, A., Zhang, B., Roth, R. A., Andersen, A. S., Kjeldsen, T., and Siddle, K. (1992) *J. Biol. Chem.* **267,** 12955–12963

36. Steele-Perkins, G., Turner, J., Edman, J. C., Hari, J., Pierce, S. B., Stover, C., Rutter, W. J., and Roth, R. A. (1988) *J. Biol. Chem.* **263,** 11486–11492

37. Ullrich, A., Gray, A., Tam, A. W., Yang-Feng, T., Tsubokawa, M., Collins, C., Henzel, W., Le Bon, T., Kathuria, S., Chen, E., Jacobs, S., Francke, U., Ramachandran, R., and Fujita-Yamagughi, Y. (1986) *EMBO J.* **5,** 2503–2512

38. Belfiore, A., Costantino, A., Frasca, F., Pandini, G., Mineo, R., Vigneri, P., Maddux, B., Goldfine, I. D., and Vigneri, R. (1996) *Mol. Endocrinol.* **10,** 1318–1326

39. Sbraccia, P., D'Adamo, M., Leonetti, F., Caiola, S., Iozzo, P., Giaccari, A., Buongiorno, A., and Tamburrano, G. (1996) *Diabetologia* **39,** 220–225

40. Klemke, R. L., Cai, S., Giannini, A. L., Gallagher, P. J., de Lanerolle, P., and Cheresh, D. A. (1997) *J. Cell Biol.* **137,** 481–492

41. Frasca, F., Vigneri, P., Vella, V., Vigneri, R., and Wang, J. Y. (2001) *Oncogene* **20,** 3845–3856

42. Koval, A. P., Karas, M., Zick, Y., and LeRoith, D. (1998) *J. Biol. Chem.* **273,** 14780–14787

43. Feller, S. M., Posern, G., Voss, J., Kardinal, C., Sakkab, D., Zheng, J., and Knudsen, B. S. (1998) *J. Cell. Physiol.* **177,** 535–552

44. Federici, M., Zucaro, L., Porzio, O., Massoud, R., Borboni, P., Lauro, D., and Sesti, G. (1996) *J. Clin. Invest.* **98,** 2887–2893

45. Federici, M., Porzio, O., Lauro, D., Borboni, P., Giovannone, B., Zucaro, L., Hribal, M. L., and Sesti, G. (1998) *J. Clin. Endocrinol. Metab.* **83,** 2911–2915

46. Spampinato, D., Pandini, G., Iuppa, A., Trischitta, V., Vigneri, R., and Frittitta, L. (2000) *J. Clin. Endocrinol. Metab.* **85,** 4219–4223

47. Frittitta, L., Sciacca, L., Catalfamo, R., Ippolito, A., Gangemi, P., Pezzino, V., Filetti, S., and Vigneri, R. (1999) *Cancer* (*Phila.*) **85,** 492–498

48. DeChiara, T. M., Efstratiadis, A., and Robertson, E. J. (1990) *Nature* **345,** 78–80

49. Louvi, A., Accili, D., and Efstratiadis, A. (1997) *Dev. Biol.* **189,** 33–48

50. Flier, J. S., Moller, D. E., Moses, A. C., O'Rahilly, S., Chaiken, R. L., Grigorescu, F., Elahi, D., Kahn, B. B., Weinreb, J. E., and Eastman, R. (1993) *J. Clin. Endocrinol. Metab.* **76,** 1533–1541